



# Ultrastructural Analysis of Cell Envelope and Accumulation of Lipid Inclusions in Clinical *Mycobacterium tuberculosis* Isolates from Sputum, Oxidative Stress, and Iron Deficiency

Srinivasan Vijay<sup>1,2</sup>, Hoang T. Hai<sup>1</sup>, Do D. A. Thu<sup>1</sup>, Errin Johnson<sup>3</sup>, Anna Pielach<sup>3</sup>, Nguyen H. Phu<sup>4</sup>, Guy E. Thwaites<sup>1,2</sup> and Nguyen T. T. Thuong<sup>1,2\*</sup>

## OPEN ACCESS

### Edited by:

Daniela De Biase,  
Sapienza Università di Roma, Italy

### Reviewed by:

Etienne Dague,  
Centre National de la Recherche  
Scientifique (CNRS), France  
Gerald Larrouy-Maumus,  
Imperial College London,  
United Kingdom

Marcos André Vannier-Santos,  
Instituto Oswaldo Cruz,  
Fundação Oswaldo Cruz, Brazil

### \*Correspondence:

Nguyen T. T. Thuong  
thuongnt@oucru.org

### Specialty section:

This article was submitted to  
Microbial Physiology and Metabolism,  
a section of the journal  
Frontiers in Microbiology

**Received:** 22 September 2017

**Accepted:** 22 December 2017

**Published:** 11 January 2018

### Citation:

Vijay S, Hai HT, Thu DDA,  
Johnson E, Pielach A, Phu NH,  
Thwaites GE and Thuong NTT (2018)  
Ultrastructural Analysis of Cell  
Envelope and Accumulation of Lipid  
Inclusions in Clinical *Mycobacterium  
tuberculosis* Isolates from Sputum,  
Oxidative Stress, and Iron Deficiency.  
*Front. Microbiol.* 8:2681.  
doi: 10.3389/fmicb.2017.02681

<sup>1</sup> Oxford University Clinical Research Unit, Ho Chi Minh City, Vietnam, <sup>2</sup> Centre for Tropical Medicine and Global Health, Nuffield Department of Medicine, University of Oxford, Oxford, United Kingdom, <sup>3</sup> Sir William Dunn School of Pathology, University of Oxford, Oxford, United Kingdom, <sup>4</sup> Hospital for Tropical Diseases, Ho Chi Minh City, Vietnam

**Introduction:** Mycobacteria have several unique cellular characteristics, such as multiple cell envelope layers, elongation at cell poles, asymmetric cell division, and accumulation of intracytoplasmic lipid inclusions, which contributes to their survival under stress conditions. However, the understanding of these characteristics in clinical *Mycobacterium tuberculosis* (*M. tuberculosis*) isolates and under host stress is limited. We previously reported the influence of host stress on the cell length distribution in a large set of clinical *M. tuberculosis* isolates ( $n = 158$ ). Here, we investigate the influence of host stress on the cellular ultrastructure of few clinical *M. tuberculosis* isolates ( $n = 8$ ) from that study. The purpose of this study is to further understand the influence of host stress on the cellular adaptations of clinical *M. tuberculosis* isolates.

**Methods:** We selected few *M. tuberculosis* isolates ( $n = 8$ ) for analyzing the cellular ultrastructure *ex vivo* in sputum and under *in vitro* stress conditions by transmission electron microscopy. The cellular adaptations of *M. tuberculosis* in sputum were correlated with the ultrastructure of antibiotic sensitive and resistant isolates in liquid culture, under oxidative stress, iron deficiency, and exposure to isoniazid.

**Results:** In sputum, *M. tuberculosis* accumulated intracytoplasmic lipid inclusions. In liquid culture, clinical *M. tuberculosis* revealed isolate to isolate variation in the extent of intracytoplasmic lipid inclusions, which were absent in the laboratory strain H37Rv. Oxidative stress, iron deficiency, and exposure to isoniazid increased the accumulation of lipid inclusions and decreased the thickness of the cell envelope electron transparent layer in *M. tuberculosis* cells. Furthermore, intracytoplasmic compartments were observed in iron deficient cells.

**Conclusion:** Our ultrastructural analysis has revealed significant influence of host stress on the cellular adaptations in clinical *M. tuberculosis* isolates. These adaptations may contribute to the survival of *M. tuberculosis* under host and antibiotic stress conditions.

Variation in the cellular adaptations among clinical *M. tuberculosis* isolates may correlate with their ability to persist in tuberculosis patients during antibiotic treatment. These observations indicate the need for further analyzing these cellular adaptations in a large set of clinical *M. tuberculosis* isolates. This will help to determine the significance of these cellular adaptations in the tuberculosis treatment.

**Keywords:** *Mycobacterium tuberculosis*, ultrastructure, intracytoplasmic lipid inclusions, cell envelope, oxidative stress, iron deficiency and mesosome

## INTRODUCTION

*Mycobacterium tuberculosis* (*M. tuberculosis*), causes tuberculosis (TB) and is a major public health problem (World Health Organization [WHO], 2015). The ability of *M. tuberculosis* cells to survive under host and antibiotic stress partly explains why *M. tuberculosis* is a successful human pathogen. Hence, cellular adaptations conferring stress tolerance in *M. tuberculosis* and in related species are an active area of research (Kieser and Rubin, 2014).

Investigations into cell biology of mycobacteria have revealed several unique characteristics in growth and division, which contributes to their survival under stress conditions (Thanky et al., 2007; Hett and Rubin, 2008; Kieser and Rubin, 2014). One such cellular structure is the complex cell envelope of mycobacteria (Brennan and Nikaido, 1995). Electron microscopy has revealed the ultrastructure of cell envelope layers in mycobacteria (Takade et al., 1983; Hoffmann et al., 2008; Zuber et al., 2008; Vijay et al., 2012). The cell envelope is essential for *M. tuberculosis* survival as it acts as a permeability barrier for the entry of antibiotics and also modulates host immune response (Jarlier and Nikaido, 1994; Briken et al., 2004; Torrelles and Schlesinger, 2010). Therefore, it is also an important drug and vaccine target (Chatterjee, 1997; Abrahams and Besra, 2016; Tima et al., 2017). The composition of cell envelope layers has been determined using cell envelope mutants (Etienne et al., 2002, 2005) and antibiotic treatments which inhibit the envelope synthesis in mycobacteria (Mdluli et al., 1998). These studies have advanced our understanding of the cell envelope role as a permeability barrier and in inhibiting phagocytosis of mycobacteria by macrophages (Mdluli et al., 1998; Etienne et al., 2002, 2005).

Another feature revealed by electron microscopy was the accumulation of intracytoplasmic lipid inclusions in mycobacteria under different host infection model systems (Peyron et al., 2008; Caire-Brandli et al., 2014; Barisch and Soldati, 2017a). In an *in vitro* human granuloma model of infection, *M. tuberculosis* cells accumulated lipid inclusions during infection of lipid loaded macrophages called foam cells (Peyron et al., 2008). Similarly, *M. avium* accumulated host-derived lipids as inclusions in foam cells and exhibited a thin cell envelope (Caire-Brandli et al., 2014). Recently, *M. marinum* was also found to have lipid inclusions derived from host lipids during the infection of *Dictyostelium* (Barisch and Soldati, 2017a). These studies have identified triacylglycerols as the major lipid in mycobacterial lipid inclusions derived from host cells (Peyron et al., 2008; Daniel et al., 2011; Caire-Brandli et al., 2014;

Barisch and Soldati, 2017a). *M. tuberculosis* and *M. smegmatis* can also accumulate lipid inclusions containing triacylglycerols under *in vitro* stress conditions independent of host cells (Garton et al., 2002; Anuchin et al., 2009; Deb et al., 2009). Several studies have shown that *M. tuberculosis* uses diverse host carbon sources such as cholesterol, pyruvate, and glucose (Pandey and Sasseti, 2008; Marrero et al., 2013; Baker et al., 2014). Utilization of such diverse carbon sources by *M. tuberculosis* contributes to its pathogenesis and persistence in the host (Pandey and Sasseti, 2008; Marrero et al., 2013; Baker et al., 2014).

Importantly, the accumulation of lipid inclusions in *M. tuberculosis* was associated with persistence, antibiotic tolerance, cavitation, and poor treatment outcome (Deb et al., 2009; Russell et al., 2009; Daniel et al., 2011; Hammond et al., 2015; Kayigire et al., 2015; Sloan et al., 2015). It is possible that this is due to growth arrest of *M. tuberculosis* and loss of antimicrobial functions by foamy macrophages leading to persistent infection (Peyron et al., 2008; Daniel et al., 2011; Caire-Brandli et al., 2014). This phenomenon may lead to clinical complications, such as relapse of infection and the emergence of antibiotic-resistant *M. tuberculosis* (Cohen et al., 2013; Sebastian et al., 2017). Thus, intracytoplasmic lipid inclusions and the cell envelope are important for the survival of *M. tuberculosis*. The understanding of these cellular characteristics and their adaptations to stress in clinical *M. tuberculosis* isolates is limited. This understanding is vital for the development of novel therapeutic targets. In our previous study, we have observed that host stresses influenced cell length distribution in a large set ( $n = 158$ ) of clinical *M. tuberculosis* isolates (Vijay et al., 2017). In this study we investigated the accumulation of lipid inclusions and cell envelope ultrastructure of *M. tuberculosis* in sputum by transmission electron microscopy (TEM). The ultrastructure of *M. tuberculosis* in sputum was compared with the ultrastructure of clinical *M. tuberculosis* isolates and H37Rv in liquid culture, and under conditions of oxidative stress, iron deficiency, and exposure to the antibiotic isoniazid.

## MATERIALS AND METHODS

### Bacterial Isolates

Six *M. tuberculosis* clinical isolates were selected from a collection of *M. tuberculosis* clinical isolates from pre-treated patients with pulmonary tuberculosis ( $n = 158$ ) in Vietnam, along with the laboratory strain H37Rv. We selected three sensitive and three

**TABLE 1** | *Mycobacterium tuberculosis* clinical strains selected for the study based on antibiotic sensitive and resistant phenotypes.

Strain name	Antibiotic resistance	<i>M. tuberculosis</i> lineages
C1	Sensitive	Indo-Oceanic
C2	STR, RIF	ND
C3	Sensitive	Indo-Oceanic
C4	STR	East Asian
C5	Sensitive	East Asian
C6	STR, RIF, INH, EMB	East Asian
H37Rv	Sensitive	Euro American

STR, streptomycin; RIF, rifampin; INH, isoniazid; EMB, ethambutol, ND, not determined.

antibiotic-resistant isolates as determined by drug susceptibility test for the electron microscopy analysis. **Table 1** presents drug sensitivity data.

## Ethics Approval Statement

Between January 2015 and October 2016, patients were recruited from two district TB control units in Ho Chi Minh City (HCMC), Vietnam. The clinical *M. tuberculosis* isolates were collected from patients before treatment. The patients were  $\geq 18$  years of age, had clinical symptoms of active pulmonary TB, which was confirmed by chest X-ray and positive sputum culture, and none of the patients were HIV positive. Written informed consent was obtained from each patient in accordance with the declaration of Helsinki. Protocols were approved by the human subjects review committees, at the Hospital for Tropical Diseases HCMC, Vietnam (124/BVBNĐ.HỒĐỒĐ) and the Oxford Tropical Research Ethics Committee, United Kingdom (OxTREC Reference: 16-14).

## Bacterial Culture

*Mycobacterium tuberculosis* isolates were cultured from sputum samples in bio safety level-3 laboratory and were stored as glycerol stocks in 7H9 media. These *M. tuberculosis* isolates were used for the experiments with a limited number of sub-culturing (approximately two to three passages) to avoid phenotypic/genotypic changes in clinical *M. tuberculosis* isolates. For mid-log culture, 50 ml culture tubes with 10 ml of 7H9T medium [7H9 broth supplemented with 10% oleic acid/albumin/dextrose/catalase (OADC) enrichment, and 0.05% Tween 80, BD Difco™] were inoculated with the clinical isolates and laboratory strain H37Rv, incubated at 37°C without shaking. The samples were processed for TEM at O.D<sub>600</sub> of 0.3–0.6.

## Drug Susceptibility Test

Drug susceptibility was performed using BACTEC™ MGIT™ 960 SIRE Kit (BD), according to manufacturer guidelines. Drug susceptibility was tested for streptomycin (1.0 μg/ml), isoniazid (0.1 μg/ml), rifampicin (1.0 μg/ml), and ethambutol (5.0 μg/ml).

## *M. tuberculosis* Lineage Identification

The lineages of the selected clinical *M. tuberculosis* isolates were determined in the previous study (Vijay et al., 2017).

## Oxidative Stress, Iron Deficiency, and Isoniazid Treatment

For TEM analysis of *M. tuberculosis* cells under different stress conditions, *M. tuberculosis* culture in 7H9T medium at O.D<sub>600</sub> 0.3–0.5 was treated with H<sub>2</sub>O<sub>2</sub> (Merk) at different concentrations, ranging from 21 to 210 mM for 48 h at 37°C and selected 21 mM H<sub>2</sub>O<sub>2</sub>-treated samples for electron microscopy (Voskuil et al., 2011). For iron deficiency, *M. tuberculosis* isolates were cultured in the presence of deferoxamine mesylate salt (DFO) (Sigma–Aldrich) at final concentrations of 100, 250, and 500 μM in 7H9T medium until the O.D<sub>600</sub> reached 0.3–0.5, with the 100 and 500 μM DFO-treated samples processed for electron microscopy (Pal et al., 2015). For isoniazid treatment, *M. tuberculosis* isolates were grown in the presence of isoniazid (Sigma–Aldrich) in 7H9T medium at a concentration of 0.015 μg/ml until the O.D<sub>600</sub> reached 0.3–0.5. All treated and untreated control isolates, along with about 500 μl of sputum with high density of acid fast bacilli (3+) as observed by microscopy from two pulmonary tuberculosis patients, were then processed for TEM.

## Transmission Electron Microscopy

*Mycobacterium tuberculosis* cells were fixed as described previously (Vijay et al., 2012). *M. tuberculosis* cells were harvested by centrifugation and fixed in 1% (vol/vol) osmium tetroxide (Sigma–Aldrich) and 0.15 M sodium cacodylate buffer (pH 7.2) (Sigma–Aldrich) for 1 h at room temperature. After this samples were washed once with the same buffer, and post fixed for 2 h at room temperature in 0.15 M cacodylate buffer (pH 7.2) containing 2% (wt/vol) tannic acid and 2% (vol/vol) glutaraldehyde (both from Sigma–Aldrich). Samples were then washed once with 0.15 M cacodylate buffer and then refixed in 1% (vol/vol) osmium tetroxide overnight at 4°C and stored at 4°C for 2–4 weeks before further processing. Next the samples were washed with water and cells were re-suspended in 4% low melting point agarose, spun down, and stored at 4°C for few minutes. These samples were cut into small fragments of less than 1 mm<sup>3</sup> and stained with 0.5% uranyl acetate overnight and washed with water. Subsequent steps were performed using a Leica EM TP automated processing unit (Leica Microsystems). Samples were dehydrated in a graded series of ice cold ethanol (Merck) and then infiltrated with epoxy resin (Taab Low Viscosity Resin, Taab Laboratories) as follows: 25% resin in ethanol for 2 h, 50% resin for 3 h, 75% resin for 2 h, then 100% resin over 48 h with several changes of resin. Samples were polymerized in beam capsules at 60°C for 48 h. Ultrathin sections (90 nm) were obtained using a Leica UC7 Ultramicrotome and a Diatome Diamond Knife (Leica microsystems and Diatome). Sections were transferred to formvar coated 100 mesh Cu grids and post-stained with Reynolds' lead citrate (Reynolds, 1963). Sections were imaged on an FEI Tecnai 12 Transmission Electron Microscope operated at 120 kV using a Gatan OneView digital camera. In each condition approximately 100 *M. tuberculosis* cells per sample were observed, except sample S2 ( $n = 10$  cells). Cell envelope layer measurements were carried out using ImageJ (Schneider et al., 2012).

## RESULTS

### *M. tuberculosis* in Sputum Displayed Triple Layered Cell Envelope and Accumulation of Intracytoplasmic Lipid Inclusions

Initially, we investigated *M. tuberculosis* cell envelope ultrastructure and lipid inclusions in pulmonary tuberculosis patient's sputum samples. The ultrastructure of these cells displayed a triple layered cell envelope which could be clearly distinguished as consisting of an electron dense outer layer (OL), electron transparent layer (ETL), and peptidoglycan layer (PGL) (Figure 1). *M. tuberculosis* cells in sputum were identified by the characteristic triple layered cell envelope of mycobacteria and distinguished from other bacteria present in the sputum (Figures 1A–C). *M. tuberculosis* cells revealed the accumulation of intracytoplasmic lipid inclusions in sputum sample S1 (Figure 1A and Table 2). The ETL of the cell envelope had an average thickness of 10.7 nm ( $\pm 9$  nm) in one of the patient sputum sample (S1) and 40 nm ( $\pm 38$  nm) in *M. tuberculosis* cells from another patient sputum sample (S2, Figure 1B). This revealed that *M. tuberculosis* cells in human hosts accumulate lipid inclusions and that envelope ultrastructure varies between hosts.

### Strain-to-Strain Variation in Accumulation of Intracytoplasmic Lipid Inclusions among Clinical *M. tuberculosis* Isolates in Mid-Log Culture Condition

We analyzed the cellular ultrastructure of six clinical *M. tuberculosis* isolates (C1–C6) along with H37Rv under mid-log culture condition (Figure 2A). Major cellular ultrastructural features of *M. tuberculosis* isolates include the triple layered cell envelope, nucleoid, and cytoplasm. These features were similar in both sensitive (C1, C3, and C5) and resistant (C2, C4, and C6) *M. tuberculosis* isolates (Figures 2A,B). We also observed mild (Figure 2A and Table 2, C1, C2, C4, and C5) to extensive (Figure 2A and Table 2, C3) accumulation of cytoplasmic lipid inclusions in clinical *M. tuberculosis* isolates, but not in H37Rv and C6 (Figure 2A and Table 2). All *M. tuberculosis* isolates in mid-log condition had an ETL of average thickness 31.7 nm ( $\pm 13.1$  nm) (Supplementary Figure S1A). We also observed high variation in ETL thickness in the same cell and between different *M. tuberculosis* cells (Supplementary Figure S1A). Based on these *ex vivo* and *in vitro* ultrastructure of clinical *M. tuberculosis* isolates we further analyzed the cellular adaptations under different stress conditions.

### Accumulation of Intracytoplasmic Lipid Inclusions Increased in Oxidative, Iron Deficiency, and Antibiotic Stresses

We observed *M. tuberculosis* cells with reduced acid fast staining and beaded appearance in sputum, oxidative stress, iron

deficiency, and isoniazid treatment (Figure 3,  $n \sim 100$ –300 cells), and then we characterized the ultrastructure of *M. tuberculosis* under these conditions (Figure 4). H<sub>2</sub>O<sub>2</sub> and isoniazid treatment resulted in a significant accumulation of intracytoplasmic lipid inclusions in clinical *M. tuberculosis* isolate C1 (Figures 4A,B and Table 2), but not in H37Rv and C4 (Figures 4A,B and Table 2). H37Rv and clinical *M. tuberculosis* isolates exposed to 100  $\mu$ M DFO did not accumulate lipid inclusions (Figure 4C and Table 2) while all isolates treated with 500  $\mu$ M DFO exhibited accumulation of lipid inclusions (Figure 4C and Table 2). Both H<sub>2</sub>O<sub>2</sub> and DFO treatments also resulted in a thinner ETL, with thickness of 13 ( $\pm 11$  nm) and 10.5 nm ( $\pm 4$  nm), respectively, in *M. tuberculosis* cell envelope as compared to untreated mid-log control (Figure 4D compared to Figure 2B,  $P < 0.0001$  Mann–Whitney *U*-test; Supplementary Figures S1B,C). Similar to the observations in *M. tuberculosis* cells from sputum, different host and antibiotic stresses increased the accumulation of intracytoplasmic lipid inclusions and reduced the cell envelope ETL in *M. tuberculosis* isolates.

### Unique Intracytoplasmic Compartment Observed in *M. tuberculosis* Cells under Iron Deficiency

In addition to the cellular adaptations observed above in different stress conditions, we also observed unique intracytoplasmic compartments in iron-deficient *M. tuberculosis* cells. This compartment was only observed in *M. tuberculosis* grown in the presence of 500  $\mu$ M DFO and not in cells grown in 100  $\mu$ M DFO and or the mid-log controls (Figure 5). Single intracytoplasmic compartments were observed in all three strains used in this experiment, H37Rv and clinical *M. tuberculosis* isolates (C1, C4), under iron deficiency ( $n = 50$  cells observed in each strain) (Figure 5A). The average size of this compartment was 250 nm ( $\pm 50$  nm,  $n = 30$  cells in total) (Figure 5B). At high magnification, we also observed membrane-like structure surrounding these intracytoplasmic compartments, some of which contained small circular units of diameter 17.4 nm ( $\pm 3.6$  nm) (Figure 5C).

## DISCUSSION

We analyzed the lipid inclusions and cell envelope layers in clinical *M. tuberculosis* isolates *ex vivo* in sputum representing the host environment. We then compared this with the ultrastructure of clinical *M. tuberculosis* isolates and H37Rv in liquid culture and under different *in vitro* stress conditions. This revealed the accumulation of intracytoplasmic lipid inclusions in clinical *M. tuberculosis* isolates as a cellular adaptation in sputum, liquid culture, and under stress conditions. Analysis of six clinical *M. tuberculosis* isolates revealed isolate-to-isolate variation in the extent of lipid inclusions in mid-log culture and its increased accumulation under stress conditions. The thickness of *M. tuberculosis* cell envelope ETL was significantly reduced under different stress conditions. Formation of an intracytoplasmic compartment in *M. tuberculosis* cells was also observed under iron deficiency.

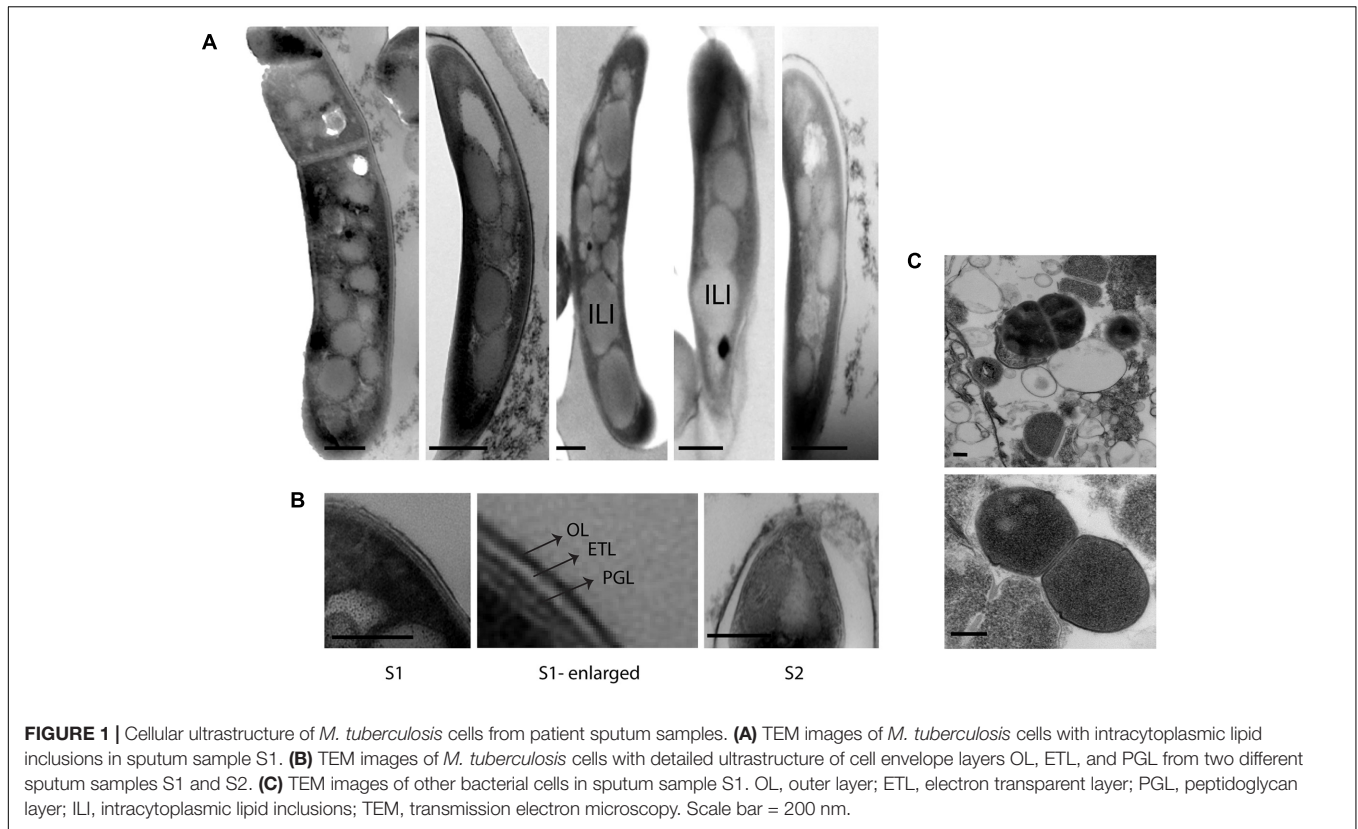


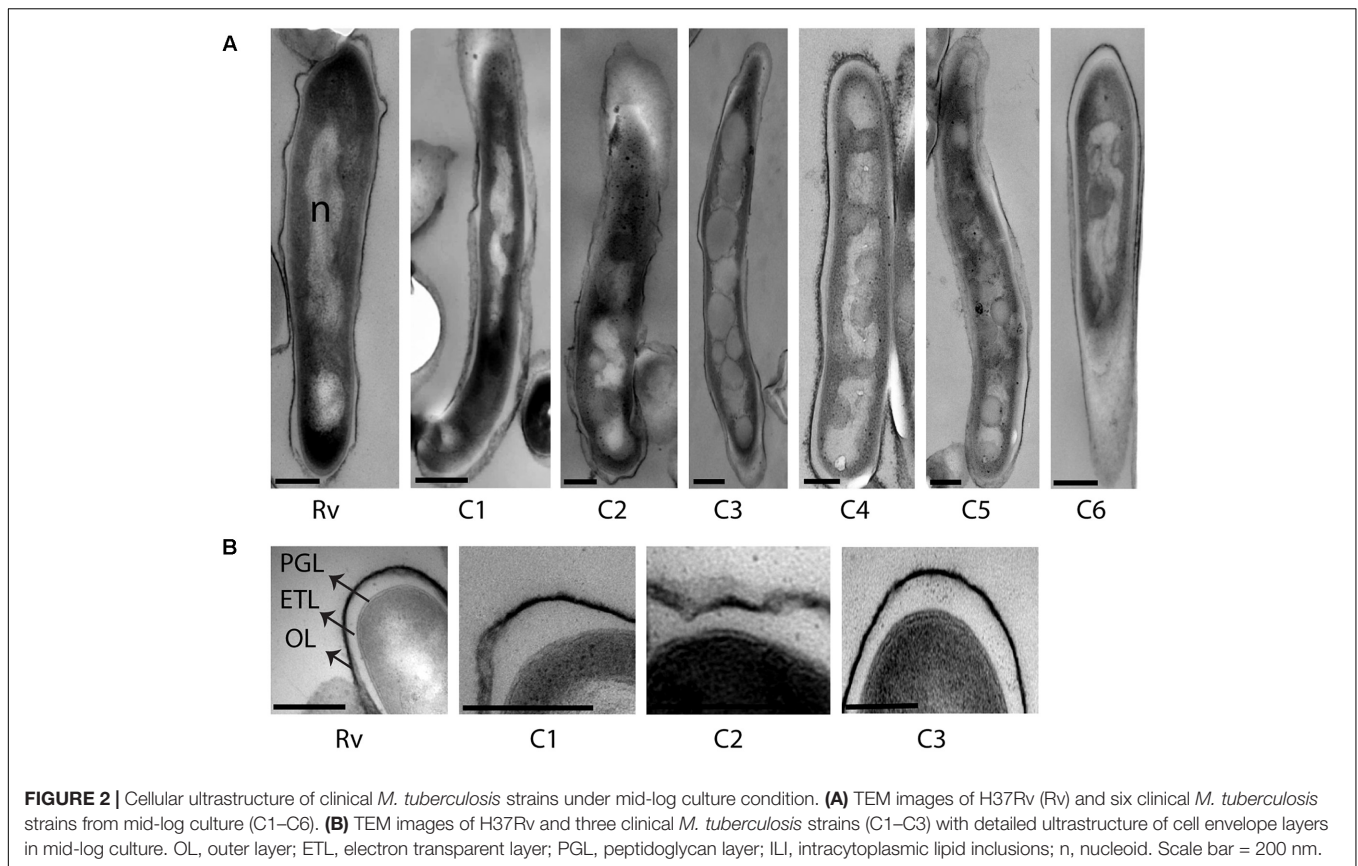
**FIGURE 1 |** Cellular ultrastructure of *M. tuberculosis* cells from patient sputum samples. **(A)** TEM images of *M. tuberculosis* cells with intracytoplasmic lipid inclusions in sputum sample S1. **(B)** TEM images of *M. tuberculosis* cells with detailed ultrastructure of cell envelope layers OL, ETL, and PGL from two different sputum samples S1 and S2. **(C)** TEM images of other bacterial cells in sputum sample S1. OL, outer layer; ETL, electron transparent layer; PGL, peptidoglycan layer; ILI, intracytoplasmic lipid inclusions; TEM, transmission electron microscopy. Scale bar = 200 nm.

*Mycobacterium tuberculosis* cells with lipid inclusions have been associated with foamy macrophages and unfavorable treatment outcome in tuberculosis patients (Garton et al., 2002; Peyron et al., 2008; Kayigire et al., 2015; Sloan et al., 2015). In the present study, clinical *M. tuberculosis* isolates displayed lipid inclusions even in liquid culture, which was not observed in the laboratory strain H37Rv. Similarly, *M. avium* and *M. marinum* also do not accumulate lipid inclusions in macrophages and the extracellular environment, respectively (Caire-Brandli et al., 2014; Barisch and Soldati, 2017a). This indicates that accumulation of lipid inclusions is a more

prominent cellular adaptation in clinical *M. tuberculosis* isolates compared to laboratory strains of mycobacteria. Supporting this, we also observed increased accumulation of lipid inclusions under both oxidative stress and sub-inhibitory concentration of isoniazid only in clinical *M. tuberculosis* isolates. Isoniazid can also induce oxidative stress and may therefore link these findings (Timmins and Deretic, 2006). It will be interesting to study how other antibiotic treatments influences the accumulation of lipid inclusions in clinical *M. tuberculosis* isolates, as its accumulation may have a role in *M. tuberculosis* persistence to antibiotics (Hammond et al., 2015; Kayigire et al., 2015; Sloan et al., 2015).

**TABLE 2 |** Quantification of intracytoplasmic lipid inclusions (ILI) in *M. tuberculosis* isolates from the study ( $n \sim 100$  cells in each isolate/condition, except S2,  $n = 10$  cells).

Growth condition	Sputum (ex vivo)		Mid-log (in vitro)							
	S1	S2	Rv	C1	C2	C3	C4	C5	C6	
Average number of ILI per cell	4 (±2)	0	0	2 (±1)	2 (±1)	6 (±3)	4 (±1)	4 (±2)	0	
Percentage of cells with ILI	90%	0%	0%	10%	5%	90%	80%	14%	0%	
Average size of ILI (nm)	250 (±150)	NA	NA	65 (±25)	100 (±75)	250 (±150)	150 (±50)	120 (±40)	NA	
Stress conditions	H <sub>2</sub> O <sub>2</sub>			INH			DFO			
	Rv-H	C1-H	C4-H	Rv-I	C1-I	Rv-D1	Rv-D2	C1-D1	C1-D2	C4-D2
Average number of ILI per cell	2 (±1)	6 (±3)	4 (±2)	0	4 (±2)	0	5 (±3)	2 (±1)	14 (±7)	11 (±5)
Percentage of cells with ILI	1%	98%	50%	0%	55%	0	99%	15%	100%	100%
Average size of ILI (nm)	70 (±30)	250 (±130)	100 (±40)	NA	80 (±20)	NA	130 (±100)	70 (±50)	140 (±70)	170 (±120)



We observed increased accumulation of lipid inclusions in *M. tuberculosis* cells at 500  $\mu$ M DFO compared to 100  $\mu$ M DFO-treated cells under iron deficiency. DFO concentration-dependent accumulation of lipid inclusions were found in both clinical *M. tuberculosis* isolates and H37Rv. Supporting these observations it has also been reported that iron deficiency and oxidative stress can induce lipid accumulation in mycobacteria, which depends on host foamy macrophages (Bacon et al., 2007; Peyron et al., 2008). Host oxidative stress generates oxidized low-density lipoproteins, and oxygenated mycolic acids present in *M. tuberculosis*; both can trigger the differentiation of host macrophages into foamy cells (Peyron et al., 2008; Palanisamy et al., 2012). This in turn facilitates the accumulation of lipid inclusions in *M. tuberculosis* cells and provides a protective niche for its survival. Our host stress models were based on *in vitro* culture lacking foamy macrophages. Hence, accumulation of lipid inclusions in our host stress models in *M. tuberculosis* cells may have derived lipids from oleic acids present in the culture media, as seen in case of *M. smegmatis* (Garton et al., 2002; Anuchin et al., 2009).

Oxidative stress was also a co-factor in all of the stress conditions where we observed the increased accumulation of lipid inclusions in *M. tuberculosis* cells (Rodriguez and Smith, 2003; Timmins and Deretic, 2006). Transcriptional adaptation of *M. tuberculosis* in macrophages and under *in vitro* stress conditions strongly correlates with the ultrastructural adaptations observed here, indicating that under host stress

*M. tuberculosis* shifts to a fatty acid-based metabolism (Schnappinger et al., 2003). Enzymes involved in fatty acid metabolism are also essential for *in vivo* growth and virulence (Munoz-Elias and McKinney, 2005; Reed et al., 2007). The accumulation of lipid inclusions is implicated in *M. tuberculosis* cell division arrest and induction of antibiotic tolerant dormant phenotype (Daniel et al., 2011; Caire-Brandli et al., 2014). This needs to be reinvestigated as our study shows that lipid inclusions *per se* may not inhibit cell division in *M. tuberculosis*. We observed *M. tuberculosis* cells with lipid inclusions growing in mid-log culture and under iron deficiency, similar to the growth observed in *M. marinum* with lipid inclusions (Barisch and Soldati, 2017a). It is possible that accumulation of lipids being a cellular adaptation that can facilitate *M. tuberculosis* entry into, and survival during dormancy (Barisch and Soldati, 2017b).

The unique triple layered cell envelope, reported in several laboratory mycobacterial strains and in clinical strains of *M. tuberculosis* (Takade et al., 1983; Brennan and Nikaido, 1995; Velayati et al., 2009; Vijay et al., 2012), was also observed in all of the clinical *M. tuberculosis* isolates in the present study. The ultrastructure of triple layered cell envelope from our study was also similar to the cell envelope ultrastructure of *M. tuberculosis* processed by cryofixation and rapid freeze substitution (Yamada et al., 2010, 2015). We also observed tearing of resin around *M. tuberculosis* cells in sputum, as observed in TEM images of *M. marinum* granulomas and *M. tuberculosis*

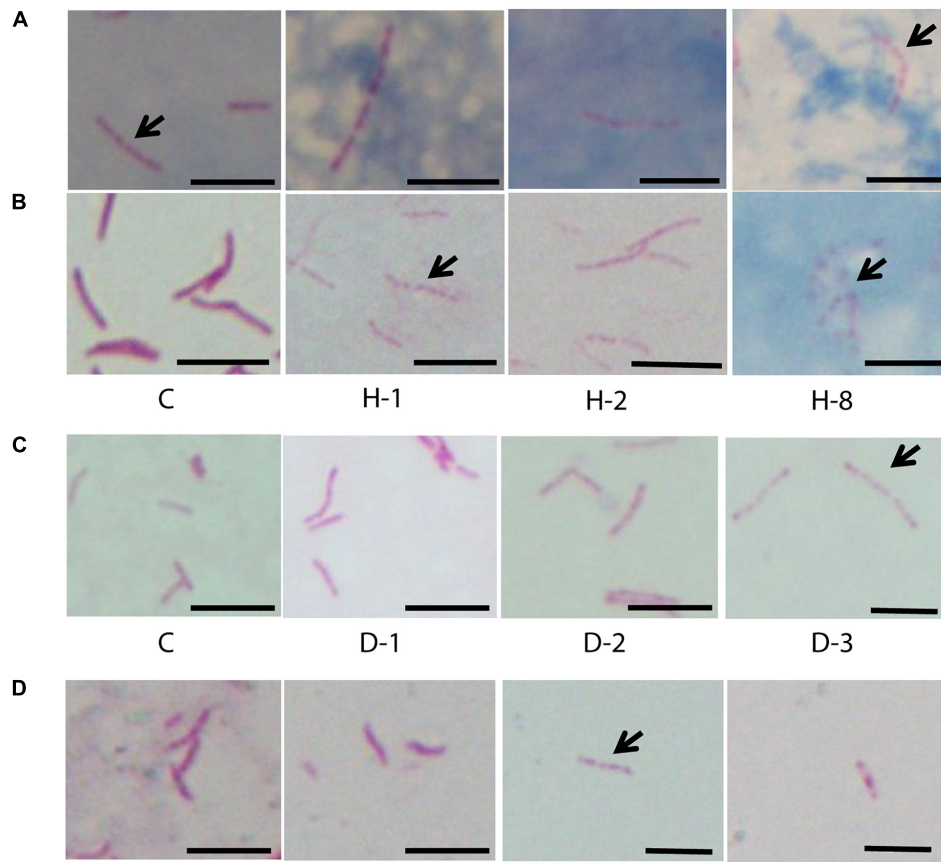


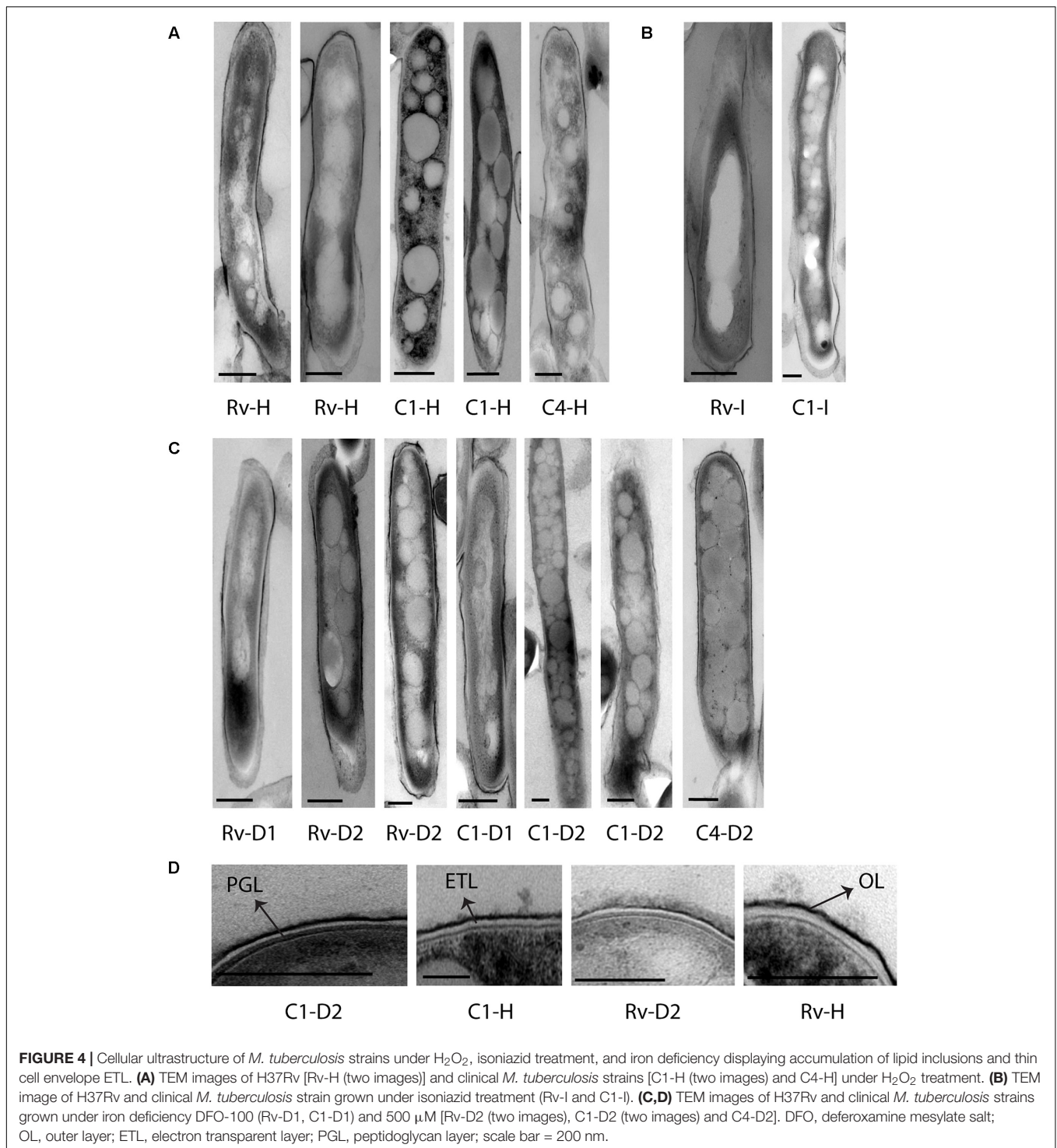
**FIGURE 3 |** Acid fast staining of *M. tuberculosis* cells in sputum, oxidative stress, iron deficiency, and isoniazid treatment. **(A)** Four sputum samples with *M. tuberculosis* cells ( $n \sim 100$  cells). **(B)** Clinical *M. tuberculosis* strain treated with different concentrations of  $H_2O_2$  for oxidative stress and **(C)** DFO for iron deficiency ( $n = 300$  cells). **(D)** Clinical *M. tuberculosis* strains grown in the presence of isoniazid ( $0.015 \mu\text{g/ml}$ ) ( $n \sim 100$  cells). C, untreated control;  $H_2O_2$  concentrations used are 21 (H-1), 42 (H-2), and 168 mM (H-8) and the concentrations of DFO are 100 (D-1), 250 (D-2), and 500  $\mu\text{M}$  (D-3), arrow indicates beaded cells and scale bar = 5  $\mu\text{m}$ .

cells (Bouley et al., 2001; Vijay et al., 2014). The thickness of the triple layers under mid-log growth conditions was consistent across the six clinical *M. tuberculosis* isolates and H37Rv used here. However, under stress conditions like sputum, oxidative stress, and iron deficiency, we observed a significant reduction in the thickness of cell envelope ETL, although the extent of this reduction varied between the two sputum samples despite a similar bacterial load. These findings suggest that the ETL can be reduced in thickness under host stress, which may vary from patient to patient. This needs to be investigated in a greater number of patients and correlated with aspects such as severity of tuberculosis symptoms and persistence to understand the clinical significance of such adaptations.

The ETL is mainly composed of lipids like mycolic acids (Mdluli et al., 1998; Wang et al., 2000) and transcriptional analysis of *M. tuberculosis* cells under host stress also indicate cell envelope remodeling and fatty acid degradation (Schnappinger et al., 2003). Cell envelope lipids are also involved in host immune modulation and virulence of *M. tuberculosis* strains (Karakousis et al., 2004; Makinoshima and Glickman, 2005). It has also been observed that under different stress conditions

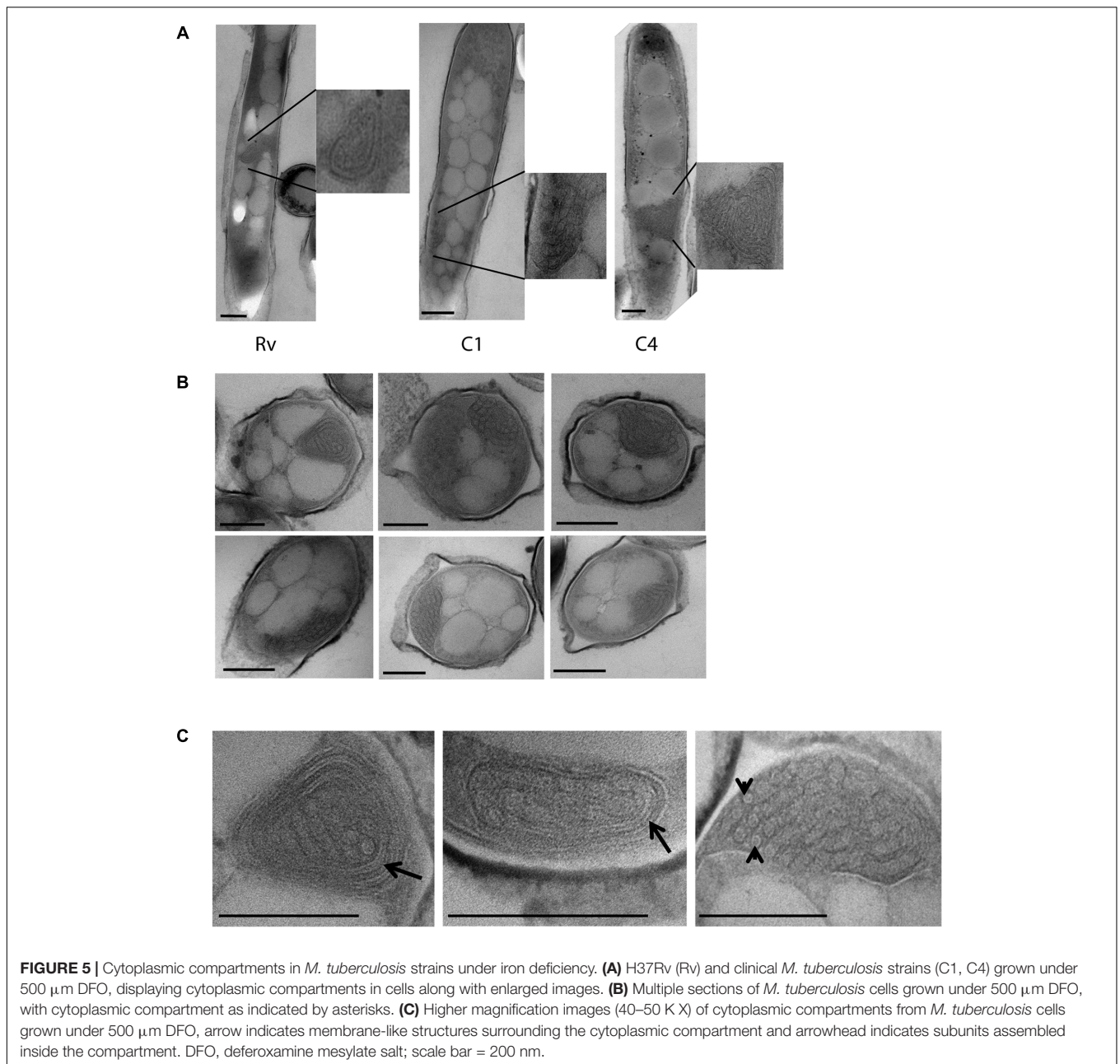
*M. tuberculosis* loses acid fastness due to loss of cell envelope lipids and it is associated with dormancy and antibiotic tolerance (Bhatt et al., 2007; Deb et al., 2009). We also observed reduced acid fast staining and *M. tuberculosis* cells with acid fast stained cytoplasmic beads in oxidative stress and iron deficiency. Such cells were also observed in some sputum samples and under isoniazid treatment, these observations strongly correlate with the ultrastructural adaptations such as reduced ETL and accumulation of lipid inclusions in our study. Further investigations are needed to understand the role of reduced cell envelope lipids on the accumulation of intracytoplasmic lipid inclusions in *M. tuberculosis*.

Reduction in the envelope lipids may enhance the permeability of cell envelope and influence the susceptibility of *M. tuberculosis* to antibiotics. Cell envelope modifications and enhanced antibiotic susceptibility in *M. smegmatis* have been observed under iron deficiency (Pal et al., 2015). Triacylglycerol is also a component of *M. tuberculosis* cell envelope and loss of acid fastness is observed under iron deficiency and in hypoxia (Rastogi et al., 2017). Such cell envelope modifications accompany non-replicative persistence and antibiotic tolerance of *M. tuberculosis*



*in vitro* (Rastogi et al., 2017). These observations indicate the influence of host factors on cellular adaptations in *M. tuberculosis* and antibiotic susceptibility. As there are multiple host factors and complex interactions influencing antibiotic susceptibility, this needs to be investigated further to identify the factors that can enhance susceptibility to antibiotics. There was significant variation in the accumulation of lipid inclusions

in clinical *M. tuberculosis* isolates in mid-log culture. Such differences between *M. tuberculosis* isolates may have a clinical significance in persistence against host stress and antibiotics. Hence, variations in cellular adaptations need to be correlated with persistence and antibiotic tolerance among clinical *M. tuberculosis* isolates to understand its role in treatment failure.



Beijing lineage was shown to accumulate triacylglycerides and has triacylglyceride synthase gene (Rv 3130c) upregulated during *in vitro* growth (Reed et al., 2007). This gene is a member of DosR regulon, and some of the regulon genes are constitutively overexpressed in Beijing lineage (Domenech et al., 2017). DosR and WhiB3 have been shown to modulate lipid accumulation in *M. tuberculosis* (Singh et al., 2009), and also contribute to bacilli adaptation to hypoxia and redox stresses, respectively (Park et al., 2003; Saini et al., 2004; Singh et al., 2009). These proteins may play a role in the accumulation of lipid inclusions under oxidative stress and iron deficiency in clinical *M. tuberculosis* isolates. The mechanism of formation of lipid inclusions in mycobacteria also involves interactions with host lipid droplets and membrane

phospholipids (Barisch and Soldati, 2017b). Thus, host stresses may induce significant cell biological adaptations in clinical *M. tuberculosis* isolates; its molecular mechanism needs to be further investigated.

In addition to reduction in the thickness of ETL and accumulation of lipid inclusions in *M. tuberculosis* cells, we also observed intracytoplasmic compartments under iron deficiency. These compartments were approximately 200 nm in size and were specifically observed in all *M. tuberculosis* isolates cultured under 500  $\mu\text{M}$  DFO. It is possible that these compartments are mesosomes as observed in bacteria treated with antibiotics (Santhana Raj et al., 2007; Li et al., 2008). Studies have also shown the formation of intracellular compartments which accumulate

H<sub>2</sub>O<sub>2</sub> under cellular damage (Ebersold et al., 1981; Li et al., 2008; Xin et al., 2014). Mesosomes and other such intracellular structures are considered as ultrastructural artifact induced under chemical fixation and dehydration process, and these are not observed under cryo-electron microscopy lacking such fixation (Pillhofer et al., 2010). In this study we have used primary fixation with osmium tetroxide for 1 h, and post-fixation with glutaraldehyde for 2 h. There is a possibility of such chemical fixation inducing the formation of intracellular structures, specifically under stress conditions. Cellular adaptations under iron deficiency may increase the probability of formation of such structures during chemical fixation, as we observed them only in *M. tuberculosis* cells under iron deficiency. In cryoelectron microscopy cells are imaged at frozen-hydrated state without chemical fixation or dehydration of cells and can avoid much of the fixation artifacts (Pillhofer et al., 2010). Cytoplasmic structure termed as stack has been reported in slow growing *Pseudomonas deceptionensis* M1 by TEM and also confirmed by cryo-electron microscopy (Delgado et al., 2013). If confirmed to be a true cellular structure by cryoelectron microscopy and specific for *M. tuberculosis* in iron deficiency. These compartments probably may have a role in iron storage.

Iron limitation has been a common host defense encountered by *M. tuberculosis*; hence, it has evolved mechanisms to sequester iron from the host by using siderophores like mycobactin (Rodriguez and Smith, 2003; Ratledge, 2004). Inside *M. tuberculosis* cells bacterioferritins BfrA and BfrB function as iron storage proteins. Recent observations have shown that BfrB can be encapsulated by the protein encapsulin to form nanocompartments *in vitro* (Reddy et al., 2012; Contreras et al., 2014). We observed arrangement of units with size ~20 nm inside these intracytoplasmic compartments in *M. tuberculosis* cells, which is similar in size to the encapsulin observed *in vitro* (Contreras et al., 2014). These observations suggest that these intracytoplasmic compartments may be encapsulin-based nanocompartments in *M. tuberculosis*. They may be used to isolate excess of iron from generating oxidative cellular damage or a similar protective function under stress (Contreras et al., 2014). Iron storage has been essential for *M. tuberculosis* survival and virulence, hence has also been a potential novel drug target (Pandey and Rodriguez, 2012). It is important to investigate further the nature of these intracytoplasmic compartments in avirulent laboratory strains by cryo-electron microscopy and its role in *M. tuberculosis* survival under iron deficiency. Recent observations further implicate survival of *M. tuberculosis* in iron

deficiency and accumulation of lipid inclusions to antibiotic tolerance and persistence (Baron et al., 2017; Kurthkoti et al., 2017).

In summary, we were able to demonstrate the major cellular adaptations of clinical *M. tuberculosis* isolates to host and antibiotic stress conditions. Further investigation of these cellular adaptations and their role in *M. tuberculosis* survival under stress is important. These will aid in our understanding of the ability of *M. tuberculosis* cells to persist during host and antibiotic stress. The variations in cellular response among clinical *M. tuberculosis* isolates may be associated with the persistence and treatment outcome among patients.

## AUTHOR CONTRIBUTIONS

SV, NT, GT, NP, and EJ conceived and designed the experiments. SV, HH, and DT did the experiments. SV and AP did TEM analysis. SV, NT, GT, EJ, and AP analyzed and interpreted the data. SV, HH, DT, NP, NT, GT, AP, and EJ drafted and revised the manuscript and approved the final version.

## FUNDING

This work was supported by the Wellcome Trust Training Fellowship in Public Health and Tropical Medicine (grant 097124/Z/11/Z to NT); the Wellcome Trust supporting the Major Overseas Program in Vietnam (grant 106680/Z/14/Z to GT).

## ACKNOWLEDGMENTS

We acknowledge the work of staff from the District TB units in Districts 4 and 8, HCMC, particularly Drs. Pham Thi Thuy Lieu and Nguyen Van Thom, who initially diagnosed and studied the patients. We would like to thank all patients who participated in this study.

## SUPPLEMENTARY MATERIAL

The Supplementary Material for this article can be found online at: <https://www.frontiersin.org/articles/10.3389/fmicb.2017.02681/full#supplementary-material>

## REFERENCES

- Abrahams, K. A., and Besra, G. S. (2016). Mycobacterial cell wall biosynthesis: a multifaceted antibiotic target. *Parasitology* doi: 10.1017/S0031182016002377 [Epub ahead of print].
- Anuchin, A. M., Mulyukin, A. L., Suzina, N. E., Duda, V. I., El-Registan, G. I., and Kaprelyants, A. S. (2009). Dormant forms of *Mycobacterium smegmatis* with distinct morphology. *Microbiology* 155(Pt 4), 1071–1079. doi: 10.1099/mic.0.023028-0
- Bacon, J., Dover, L. G., Hatch, K. A., Zhang, Y., Gomes, J. M., Kendall, S., et al. (2007). Lipid composition and transcriptional response of *Mycobacterium tuberculosis* grown under iron-limitation in continuous culture: identification of a novel wax ester. *Microbiology* 153(Pt 5), 1435–1444. doi: 10.1099/mic.0.2006/004317-0
- Baker, J. J., Johnson, B. K., and Abramovitch, R. B. (2014). Slow growth of *Mycobacterium tuberculosis* at acidic pH is regulated by phoPR and host-associated carbon sources. *Mol. Microbiol.* 94, 56–69. doi: 10.1111/mmi.12688

- Barisch, C., and Soldati, T. (2017a). *Mycobacterium marinum* degrades both triacylglycerols and phospholipids from its *Dictyostelium* host to synthesise its own triacylglycerols and generate lipid inclusions. *PLoS Pathog.* 13:e1006095. doi: 10.1371/journal.ppat.1006095
- Barisch, C., and Soldati, T. (2017b). Breaking fat! How mycobacteria and other intracellular pathogens manipulate host lipid droplets. *Biochimie* 141, 54–61. doi: 10.1016/j.biochi.2017.06.001
- Baron, V. O., Chen, M., Clark, S. O., Williams, A., Hammond, R. J. H., Dholakia, K., et al. (2017). Label-free optical vibrational spectroscopy to detect the metabolic state of *M. tuberculosis* cells at the site of disease. *Sci. Rep.* 7:9844. doi: 10.1038/s41598-017-10234-z
- Bhatt, A., Fujiwara, N., Bhatt, K., Gurcha, S. S., Kremer, L., Chen, B., et al. (2007). Deletion of kasB in *Mycobacterium tuberculosis* causes loss of acid-fastness and subclinical latent tuberculosis in immunocompetent mice. *Proc. Natl. Acad. Sci. U.S.A.* 104, 5157–5162. doi: 10.1073/pnas.0608654104
- Bouley, D. M., Ghori, N., Mercer, K. L., Falkow, S., and Ramakrishnan, L. (2001). Dynamic nature of host-pathogen interactions in *Mycobacterium marinum* granulomas. *Infect. Immun.* 69, 7820–7831. doi: 10.1128/IAI.69.12.7820-7831.2001
- Brennan, P. J., and Nikaido, H. (1995). The envelope of mycobacteria. *Annu. Rev. Biochem.* 64, 29–63. doi: 10.1146/annurev.bi.64.070195.000333
- Briken, V., Porcelli, S. A., Besra, G. S., and Kremer, L. (2004). Mycobacterial lipoarabinomannan and related lipoglycans: from biogenesis to modulation of the immune response. *Mol. Microbiol.* 53, 391–403. doi: 10.1111/j.1365-2958.2004.04183.x
- Caire-Brandli, I., Papadopoulos, A., Malaga, W., Marais, D., Canaan, S., Thilo, L., et al. (2014). Reversible lipid accumulation and associated division arrest of *Mycobacterium avium* in lipoprotein-induced foamy macrophages may resemble key events during latency and reactivation of tuberculosis. *Infect. Immun.* 82, 476–490. doi: 10.1128/IAI.01196-13
- Chatterjee, D. (1997). The mycobacterial cell wall: structure, biosynthesis and sites of drug action. *Curr. Opin. Chem. Biol.* 1, 579–588. doi: 10.1016/S1367-5931(97)80055-5
- Cohen, N. R., Lobritz, M. A., and Collins, J. J. (2013). Microbial persistence and the road to drug resistance. *Cell Host Microbe.* 13, 632–642. doi: 10.1016/j.chom.2013.05.009
- Contreras, H., Joens, M. S., McMath, L. M., Le, V. P., Tullius, M. V., Kimmey, J. M., et al. (2014). Characterization of a *Mycobacterium tuberculosis* nanocompartment and its potential cargo proteins. *J. Biol. Chem.* 289, 18279–18289. doi: 10.1074/jbc.M114.570119
- Daniel, J., Maamar, H., Deb, C., Sirakova, T. D., and Kolattukudy, P. E. (2011). *Mycobacterium tuberculosis* uses host triacylglycerol to accumulate lipid droplets and acquires a dormancy-like phenotype in lipid-loaded macrophages. *PLoS Pathog.* 7:e1002093. doi: 10.1371/journal.ppat.1002093
- Deb, C., Lee, C. M., Dubey, V. S., Daniel, J., Abomoelak, B., Sirakova, T. D., et al. (2009). A novel *in vitro* multiple-stress dormancy model for *Mycobacterium tuberculosis* generates a lipid-loaded, drug-tolerant, dormant pathogen. *PLoS ONE* 4:e6077. doi: 10.1371/journal.pone.0006077
- Delgado, L., Carrion, O., Martinez, G., Lopez-Iglesias, C., and Mercade, E. (2013). The stack: a new bacterial structure analyzed in the Antarctic bacterium *Pseudomonas deceptionensis* M1(T) by transmission electron microscopy and tomography. *PLoS ONE* 8:e73297. doi: 10.1371/journal.pone.0073297
- Domenech, P., Zou, J., Averback, A., Syed, N., Curtis, D., Donato, S., et al. (2017). Unique regulation of the DosR regulon in the Beijing lineage of *Mycobacterium tuberculosis*. *J. Bacteriol.* 199:e00696-16. doi: 10.1128/JB.00696-16
- Ebersold, H. R., Cordier, J. L., and Luthy, P. (1981). Bacterial mesosomes: method dependent artifacts. *Arch. Microbiol.* 130, 19–22. doi: 10.1007/BF00527066
- Etienne, G., Laval, F., Villeneuve, C., Dinadayala, P., Abouwarda, A., Zerbib, D., et al. (2005). The cell envelope structure and properties of *Mycobacterium smegmatis* mc2155: is there a clue for the unique transformability of the strain? *Microbiology* 151(Pt 6), 2075–2086.
- Etienne, G., Villeneuve, C., Billman-Jacobe, H., Astarie-Dequeker, C., Dupont, M. A., and Daffe, M. (2002). The impact of the absence of glycopeptidolipids on the ultrastructure, cell surface and cell wall properties, and phagocytosis of *Mycobacterium smegmatis*. *Microbiology* 148(Pt 10), 3089–3100. doi: 10.1099/00221287-148-10-3089
- Garton, N. J., Christensen, H., Minnikin, D. E., Adegbola, R. A., and Barer, M. R. (2002). Intracellular lipophilic inclusions of mycobacteria *in vitro* and in sputum. *Microbiology* 148(Pt 10), 2951–2958. doi: 10.1099/00221287-148-10-2951
- Hammond, R. J., Baron, V. O., Oravcova, K., Lipworth, S., and Gillespie, S. H. (2015). Phenotypic resistance in mycobacteria: is it because I am old or fat that I resist you? *J. Antimicrob. Chemother.* 70, 2823–2827. doi: 10.1093/jac/dkv178
- Hett, E. C., and Rubin, E. J. (2008). Bacterial growth and cell division: a mycobacterial perspective. *Microbiol. Mol. Biol. Rev.* 72, 126–156. doi: 10.1128/MMBR.00028-07
- Hoffmann, C., Leis, A., Niederweis, M., Plitzko, J. M., and Engelhardt, H. (2008). Disclosure of the mycobacterial outer membrane: cryo-electron tomography and vitreous sections reveal the lipid bilayer structure. *Proc. Natl. Acad. Sci. U.S.A.* 105, 3963–3967. doi: 10.1073/pnas.0709530105
- Jarlier, V., and Nikaido, H. (1994). Mycobacterial cell wall: structure and role in natural resistance to antibiotics. *FEMS Microbiol. Lett.* 123, 11–18. doi: 10.1111/j.1574-6968.1994.tb07194.x
- Karakousis, P. C., Bishai, W. R., and Dorman, S. E. (2004). *Mycobacterium tuberculosis* cell envelope lipids and the host immune response. *Cell Microbiol.* 6, 105–116. doi: 10.1046/j.1462-5822.2003.00351.x
- Kayigire, X. A., Friedrich, S. O., van der Merwe, L., Donald, P. R., and Diacon, A. H. (2015). Simultaneous staining of sputum smears for acid-fast and lipid-containing *Myobacterium tuberculosis* can enhance the clinical evaluation of antituberculosis treatments. *Tuberculosis* 95, 770–779. doi: 10.1016/j.tube.2015.08.001
- Kieser, K. J., and Rubin, E. J. (2014). How sisters grow apart: mycobacterial growth and division. *Nat. Rev. Microbiol.* 12, 550–562. doi: 10.1038/nrmicro3299
- Kurthkoti, K., Amin, H., Marakalala, M. J., Ghanny, S., Subbian, S., Sakatos, A., et al. (2017). The capacity of *Mycobacterium tuberculosis* to survive iron starvation might enable it to persist in iron-deprived microenvironments of human granulomas. *mBio* 8:e01092-17. doi: 10.1128/mBio.01092-17
- Li, X., Feng, H. Q., Pang, X. Y., and Li, H. Y. (2008). Mesosome formation is accompanied by hydrogen peroxide accumulation in bacteria during the rifampicin effect. *Mol. Cell. Biochem.* 311, 241–247. doi: 10.1007/s11010-007-9690-4
- Makinoshima, H., and Glickman, M. S. (2005). Regulation of *Mycobacterium tuberculosis* cell envelope composition and virulence by intramembrane proteolysis. *Nature* 436, 406–409. doi: 10.1038/nature03713
- Marrero, J., Trujillo, C., Rhee, K. Y., and Ehrst, S. (2013). Glucose phosphorylation is required for *Mycobacterium tuberculosis* persistence in mice. *PLoS Pathog.* 9:e1003116. doi: 10.1371/journal.ppat.1003116
- Mdluli, K., Swanson, J., Fischer, E., Lee, R. E., and Barry, C. E. III. (1998). Mechanisms involved in the intrinsic isoniazid resistance of *Mycobacterium avium*. *Mol. Microbiol.* 27, 1223–1233. doi: 10.1046/j.1365-2958.1998.00774.x
- Munoz-Elias, E. J., and McKinney, J. D. (2005). *Mycobacterium tuberculosis* isocitrate lyases 1 and 2 are jointly required for *in vivo* growth and virulence. *Nat. Med.* 11, 638–644. doi: 10.1038/nm1252
- Pal, R., Hameed, S., and Fatima, Z. (2015). Iron deprivation affects drug susceptibilities of mycobacteria targeting membrane integrity. *J. Pathog.* 2015:938523. doi: 10.1155/2015/938523
- Palanisamy, G. S., Kirk, N. M., Ackart, D. F., Obregon-Henao, A., Shanley, C. A., Orme, I. M., et al. (2012). Uptake and accumulation of oxidized low-density lipoprotein during *Mycobacterium tuberculosis* infection in guinea pigs. *PLoS ONE* 7:e34148. doi: 10.1371/journal.pone.0034148
- Pandey, A. K., and Sasseti, C. M. (2008). Mycobacterial persistence requires the utilization of host cholesterol. *Proc. Natl. Acad. Sci. U.S.A.* 105, 4376–4380. doi: 10.1073/pnas.0711159105
- Pandey, R., and Rodriguez, G. M. (2012). A ferritin mutant of *Mycobacterium tuberculosis* is highly susceptible to killing by antibiotics and is unable to establish a chronic infection in mice. *Infect. Immun.* 80, 3650–3659. doi: 10.1128/IAI.00229-12
- Park, H. D., Guinn, K. M., Harrell, M. I., Liao, R., Voskuil, M. I., Tompa, M., et al. (2003). Rv3133c/dosR is a transcription factor that mediates the hypoxic response of *Mycobacterium tuberculosis*. *Mol. Microbiol.* 48, 833–843. doi: 10.1046/j.1365-2958.2003.03474.x
- Peyron, P., Vaubourgeix, J., Poquet, Y., Levillain, F., Botanch, C., Bardou, F., et al. (2008). Foamy macrophages from tuberculous patients' granulomas constitute a nutrient-rich reservoir for *M. tuberculosis* persistence. *PLoS Pathog.* 4:e1000204. doi: 10.1371/journal.ppat.1000204

- Pilhofer, M., Ladinsky, M. S., McDowall, A. W., and Jensen, G. J. (2010). Bacterial TEM: new insights from cryo-microscopy. *Methods Cell Biol.* 96, 21–45. doi: 10.1016/S0091-679X(10)96002-0
- Rastogi, S., Singh, A. K., Chandra, G., Kushwaha, P., Pant, G., Singh, K., et al. (2017). The diacylglycerol acyltransferase Rv3371 of *Mycobacterium tuberculosis* is required for growth arrest and involved in stress-induced cell wall alterations. *Tuberculosis* 104, 8–19. doi: 10.1016/j.tube.2017.02.001
- Ratledge, C. (2004). Iron, mycobacteria and tuberculosis. *Tuberculosis* 84, 110–130. doi: 10.1016/j.tube.2003.08.012
- Reddy, P. V., Puri, R. V., Khera, A., and Tyagi, A. K. (2012). Iron storage proteins are essential for the survival and pathogenesis of *Mycobacterium tuberculosis* in THP-1 macrophages and the guinea pig model of infection. *J. Bacteriol.* 194, 567–575. doi: 10.1128/JB.05553-11
- Reed, M. B., Gagneux, S., Deriemer, K., Small, P. M., and Barry, C. E. III (2007). The W-Beijing lineage of *Mycobacterium tuberculosis* overproduces triglycerides and has the DosR dormancy regulon constitutively upregulated. *J. Bacteriol.* 189, 2583–2589. doi: 10.1128/JB.01670-06
- Reynolds, E. S. (1963). The use of lead citrate at high pH as an electron-opaque stain in electron microscopy. *J. Cell Biol.* 17, 208–212. doi: 10.1083/jcb.17.1.208
- Rodriguez, G. M., and Smith, I. (2003). Mechanisms of iron regulation in mycobacteria: role in physiology and virulence. *Mol. Microbiol.* 47, 1485–1494. doi: 10.1046/j.1365-2958.2003.03384.x
- Russell, D. G., Cardona, P. J., Kim, M. J., Allain, S., and Altare, F. (2009). Foamy macrophages and the progression of the human tuberculosis granuloma. *Nat. Immunol.* 10, 943–948. doi: 10.1038/ni.1781
- Saini, D. K., Malhotra, V., Dey, D., Pant, N., Das, T. K., and Tyagi, J. S. (2004). DevR-DevS is a bona fide two-component system of *Mycobacterium tuberculosis* that is hypoxia-responsive in the absence of the DNA-binding domain of DevR. *Microbiology* 150(Pt 4), 865–875. doi: 10.1099/mic.0.26218-0
- Santhana Raj, L., Hing, H. L., Baharudin, O., Teh Hamidah, Z., Aida Suhana, R., Nor Asiha, C. P., et al. (2007). Mesosomes are a definite event in antibiotic-treated *Staphylococcus aureus* ATCC 25923. *Trop. Biomed.* 24, 105–109.
- Schnappinger, D., Ehrst, S., Voskuil, M. I., Liu, Y., Mangan, J. A., Monahan, I. M., et al. (2003). Transcriptional adaptation of *Mycobacterium tuberculosis* within macrophages: insights into the phagosomal environment. *J. Exp. Med.* 198, 693–704. doi: 10.1084/jem.20030846
- Schneider, C. A., Rasband, W. S., and Eliceiri, K. W. (2012). NIH Image to ImageJ: 25 years of image analysis. *Nat. Methods* 9, 671–675. doi: 10.1038/nmeth.2089
- Sebastian, J., Swaminath, S., Nair, R. R., Jakkala, K., Pradhan, A., and Ajitkumar, P. (2017). *De novo* emergence of genetically resistant mutants of *Mycobacterium tuberculosis* from the persistence phase cells formed against antituberculosis drugs *in vitro*. *Antimicrob. Agents Chemother.* 61:e01343-16. doi: 10.1128/AAC.01343-16
- Singh, A., Crossman, D. K., Mai, D., Guidry, L., Voskuil, M. I., Renfrow, M. B., et al. (2009). *Mycobacterium tuberculosis* WhiB3 maintains redox homeostasis by regulating virulence lipid anabolism to modulate macrophage response. *PLoS Pathog.* 5:e1000545. doi: 10.1371/journal.ppat.1000545
- Sloan, D. J., Mwandumba, H. C., Garton, N. J., Khoo, S. H., Butterworth, A. E., Allain, T. J., et al. (2015). Pharmacodynamic modeling of bacillary elimination rates and detection of bacterial lipid bodies in sputum to predict and understand outcomes in treatment of pulmonary tuberculosis. *Clin. Infect. Dis.* 61, 1–8. doi: 10.1093/cid/civ195
- Takade, A., Takeya, K., Taniguchi, H., and Mizuguchi, Y. (1983). Electron microscopic observations of cell division in *Mycobacterium vaccae* V1. *J. Gen. Microbiol.* 129, 2315–2320. doi: 10.1099/00221287-129-7-2315
- Thanky, N. R., Young, D. B., and Robertson, B. D. (2007). Unusual features of the cell cycle in mycobacteria: polar-restricted growth and the snapping-model of cell division. *Tuberculosis* 87, 231–236. doi: 10.1016/j.tube.2006.10.004
- Tima, H. G., Al Dulayymi, J. R., Denis, O., Lehebel, P., Baols, K. S., Mohammed, M. O., et al. (2017). Inflammatory properties and adjuvant potential of synthetic glycolipids homologous to mycolate esters of the cell wall of *Mycobacterium tuberculosis*. *J. Innate Immun.* 9, 162–180. doi: 10.1159/000450955
- Timmins, G. S., and Deretic, V. (2006). Mechanisms of action of isoniazid. *Mol. Microbiol.* 62, 1220–1227. doi: 10.1111/j.1365-2958.2006.05467.x
- Torrelles, J. B., and Schlesinger, L. S. (2010). Diversity in *Mycobacterium tuberculosis* mannosylated cell wall determinants impacts adaptation to the host. *Tuberculosis* 90, 84–93. doi: 10.1016/j.tube.2010.02.003
- Velayati, A. A., Farnia, P., Ibrahim, T. A., Haroun, R. Z., Kuan, H. O., Ghanavi, J., et al. (2009). Differences in cell wall thickness between resistant and nonresistant strains of *Mycobacterium tuberculosis*: using transmission electron microscopy. *Chemotherapy* 55, 303–307. doi: 10.1159/000226425
- Vijay, S., Anand, D., and Ajitkumar, P. (2012). Unveiling unusual features of formation of septal partition and constriction in mycobacteria—an ultrastructural study. *J. Bacteriol.* 194, 702–707. doi: 10.1128/JB.06184-11
- Vijay, S., Nagaraja, M., Sebastian, J., and Ajitkumar, P. (2014). Asymmetric cell division in *Mycobacterium tuberculosis* and its unique features. *Arch. Microbiol.* 196, 157–168. doi: 10.1007/s00203-014-0953-7
- Vijay, S., Vinh, D. N., Hai, H. T., Ha, V. T. N., Dung, V. T. M., Dinh, T. D., et al. (2017). Influence of stress and antibiotic resistance on cell-length distribution in *Mycobacterium tuberculosis* clinical isolates. *Front. Microbiol.* 8:2296. doi: 10.3389/fmicb.2017.02296
- Voskuil, M. I., Bartek, I. L., Visconti, K., and Schoolnik, G. K. (2011). The response of mycobacterium tuberculosis to reactive oxygen and nitrogen species. *Front. Microbiol.* 2:105. doi: 10.3389/fmicb.2011.00105
- Wang, L., Slayden, R. A., Barry, C. E. III, and Liu, J. (2000). Cell wall structure of a mutant of *Mycobacterium smegmatis* defective in the biosynthesis of mycolic acids. *J. Biol. Chem.* 275, 7224–7229. doi: 10.1074/jbc.275.10.7224
- World Health Organization [WHO] (2015). *Global Tuberculosis Report 2015*. Geneva: World Health Organization.
- Xin, L., Lipeng, Y., Jiaju, Q., Hanqing, F., Yunhong, L., Min, Z., et al. (2014). Revisiting the mesosome as a novel site of hydrogen peroxide accumulation in *Escherichia coli*. *Curr. Microbiol.* 69, 549–553. doi: 10.1007/s00284-014-0617-5
- Yamada, H., Mitarai, S., Chikamatsu, K., Mizuno, K., and Yamaguchi, M. (2010). Novel freeze-substitution electron microscopy provides new aspects of virulent *Mycobacterium tuberculosis* with visualization of the outer membrane and satisfying biosafety requirements. *J. Microbiol. Methods* 80, 14–18. doi: 10.1016/j.mimet.2009.09.022
- Yamada, H., Yamaguchi, M., Chikamatsu, K., Aono, A., and Mitarai, S. (2015). Structome analysis of virulent *Mycobacterium tuberculosis*, which survives with only 700 ribosomes per 0.1 fl of cytoplasm. *PLOS ONE* 10:e0117109. doi: 10.1371/journal.pone.0117109
- Zuber, B., Chami, M., Houssin, C., Dubochet, J., Griffiths, G., and Daffe, M. (2008). Direct visualization of the outer membrane of mycobacteria and corynebacteria in their native state. *J. Bacteriol.* 190, 5672–5680. doi: 10.1128/JB.01919-07

**Conflict of Interest Statement:** The authors declare that the research was conducted in the absence of any commercial or financial relationships that could be construed as a potential conflict of interest.

Copyright © 2018 Vijay, Hai, Thu, Johnson, Pielach, Phu, Thwaites and Thuong. This is an open-access article distributed under the terms of the Creative Commons Attribution License (CC BY). The use, distribution or reproduction in other forums is permitted, provided the original author(s) or licensor are credited and that the original publication in this journal is cited, in accordance with accepted academic practice. No use, distribution or reproduction is permitted which does not comply with these terms.